Journal of Physics: Conference Series **500** (2014) 052003 doi:10.1088/1742-6596/500/5/052003

Study of thermite mixture consolidated by the cold gas dynamic spray process

A Bacciochini[1], G Maines[1], C Poupart[1], H Akbarnejad[1], M Radulescu[1], B Jodoin[1], F Zhang[2] and J J Lee[2]

[1] University of Ottawa, Department of Mechanical Engineering, 161 Louis Pasteur, Ottawa, ON, K1N 6N5, Canada

[2] Defence Research and Development Canada-Suffield, PO Box 4000, Stn Main, Medicine Hat, AB, T1A 8K6, Canada

E-mail: antoine.bacciochini@gmail.com

Abstract. The present study focused on the cold gas dynamic spray process for manufacturing porosity free, finely structured energetic materials with high reactivity and structural integrity. The experiments have focused the reaction between the aluminium and metal oxide, such as Al-CuO system. The consolidation of the materials used the cold gas dynamic spray technique, where the particles are accelerated to high speeds and consolidated via plastic deformation upon impact. Reactive composites are formed in arbitrary shapes with close to zero porosity and without any reactions during the consolidation phase. Reactivity of mixtures has been investigated through flame propagation analysis on cold sprayed samples and compacted powder mixture. Deflagration tests showed the influence of porosity on the reactivity.

1. Introduction

It is well known that thermites and Metastable Interstitial Materials (MIC) can be used for a variety of applications where the use of highly explosive reactive materials and their collateral effects are not desired. Applications include but are not limited to the following [1]: biological agent defeat, material destruction, blast effect enhancement, high explosive target countermeasure, metal/concrete cutting, propellant/explosive additives.

Thermite reactive mixtures are highly exothermic [2] and exhibit a wide range of reactivity. Such reactive materials are heterogeneous in nature, since they consist of two or more solid phase metals or ceramics, which need to be mixed. While significant effort has been devoted to develop methods that can help tailor the reactivity of such materials by controlling the dimension of the elemental materials, such as nano-scale assemblies [3], size refinement by ball milling [4] or physical vapor deposition of nano-layers [5], minimal effort was directed towards developing viable techniques to achieve bulk materials with structural integrity. Indeed, numerous applications require the reactive material to be consolidated in desired net-shape form. While thin films [5] and thermophoresis [6] methods appear promising for micro-scale applications, these techniques can hardly be scaled up to achieve reactive structural materials of centimeters to meters dimensions.

In a previous study, the Cold Spray deposition technique has been used to manufacture structural materials of inter-metallics with desirable reactive characteristics [4]. When combined with ball milling, net-shape samples of Ni–Al composites with 100% TMD and nano-scale intermixing of the constituents were obtained. Owing to the high thermal conductivity of the material, its reactive

properties were greatly enhanced. Measurements revealed flame speeds higher by an order of magnitude compared to those obtained with compacted powders, while the material stability to ignition was greatly improved owing to the propensity of the material to rapidly dissipate any applied heat source [4].

Thermite reactions are most often described as gasless, however the high exothermicity of the reaction can produce a fairly amount of transient gases. The current study aims to develop a spray-consolidation method whereby arbitrary shapes can be built of dimensions ranging from square centimeters to square meters and up to several millimeters thick. These composite materials are then tested to evaluate some of the mechanical properties desired for a reactive structural material, such as microhardness along samples thickness, as well as four-point bending on free-standing samples. Likewise, the reactivity of these porosity free materials is also evaluated via ignition and flame propagation experiments.

2. Experimental procedure

The raw materials used in this work were high purity aluminium powders and copper oxide (copper (II) oxide, CuO) powders, from Atlantic Engineer Equipment (NJ, USA). The CuO particles have a micron-size distribution with an average diameter of d_{10} = 1.5 μm and d_{50} = 4.1 μm, as measured by statistical analysis from SEM records, while the Al powder has been sieved below 635 meshes (−20 μm). The CuO and Al powders were mechanically mixed at the stoichiometric atomic ratio of Al–CuO (2:3)

2.1. Sample manufacturing

The powder mixtures were consolidated using the Cold Gas Dynamic Spraying (CGDS) process [7], also known as Cold Spray process, using the commercially available SST Cold-Spray system series P (from Centerline (Windsor) Ltd, Windsor, Canada). Figure 1 is a schematic of the Cold Spray process. A pressurized propellant gas is heated before flowing through a converging–diverging nozzle, where the thermal energy is converted into kinetic energy, creating a supersonic flow. The feedstock powder is injected in this flow using a pressurized carrier gas and accelerated. Upon the impact on the substrate, particles deform and build up a deposit by intense local plastic deformation in the solid state [8]. The operating parameters used are listed in table 1. In order to achieve a large range of relative densities, various test samples were also compacted at room temperature either in a 2.5×2.5×70 mm^3 channel or in a 15 mm diameter cylindrical compaction die and then cut into similar surface to volume ratio samples. The resulting average final densities ranged from 25% to 85% of the theoretical maximum density (TMD), estimated through direct measurements of mass and volume of samples. The high density samples were produced by cold spray with a size about 2.5×2.5×10 mm^3, comparable to compacted samples.

2.2. Characterization methods

The consolidated samples microstructure was observed using scanning electron microscopy (EVO MA-10, Carl Zeiss NTS GmbH, Germany) equipped with a backscattered electron (BSE) detector and an energy dispersive spectrometer (EDS) probe (INCA-x-act, Oxford Instrument, UK) for chemical analysis. The as-received powder samples were first examined. Once consolidated by the Cold Spray process, the samples were sectioned perpendicularly to the spray direction and prepared for cross-section investigation, following standard metallographic preparation techniques.

Microstructural features such as the consolidated sample thickness, porosity level, and CuO volume fraction levels were obtained from the polished samples' cross-section images, using image analysis technique (Clemex Vision-Lite software).

X-ray diffraction (XRD) patterns were recorded in a Bragg–Brentano geometry using a Siemens D5005 diffractometer equipped with incident beam monochromator. The data collection was carried out at a room temperature using monochromatic Cu Kα1 radiation (λ = 0.154056 nm) in the 2θ region between 30° and 90°, step size 0.02° 2θ and an acquisition step of 2 s.

Vickers microhardness measurements were performed on the polished cross-section of the consolidated samples using a 300 g ($HV_{0.3}$) load and a dwell time of 10 s using a Duramin-1 microhardness tester (Struers Inc., Cleveland, OH, USA).

Four-point bending tests were performed using consolidated freestanding samples (*i.e.* detached from the substrate onto which they were initially sprayed). The samples dimensions were 7.5 mm width, 50 mm length and 1 mm thick. The samples were milled and polished to remove all surface defects that could initiate crack propagation. An Instron universal testing machine, model 4482 equipped with a 1 kN static load cell has been used to assess the flexural properties. The tests were performed according to the ASTM standard D6272-10. The rate of crosshead motion was set at 1 mm/s. The average maximal flexural stress and strain as well as the flexural moduli have been measured from five samples for each powder mixture.

Bulk thermal conductivity and specific heat capacity of samples was measured using a ThermTest TPS 2500 S Thermal Constants Analyzer (ThermTest Inc., Canada). The samples used for the thermal characterization were disc shaped with a nominal diameter of 15 mm, and their relative density was about 30, 80 and 100% TMD.

Ignition and burning of the samples was carried out into air at room pressure and temperature. The samples' ignition was performed using a tungsten wire of 0.5 mm diameter and a tunable power supply, the electrical power dissipated through the hot-wire was about 200 to 250 W. Flame speed measurements were made with a Casio EX-F1 high speed camera set at 1200 fps and exposure time of 1/40,000 s. Individual frames were then extracted to measure the average flame velocity.

Table 1. Cold spray process operating parameters.

Parameters	Values
Nozzle internal exit diameter [mm]	6.2
Throat diameter [mm]	2
Throat nozzle distance [mm]	120
Standoff distance [mm]	10
Traverse speed [mm/s]	10
Working gas	Helium
Stagnation temperature [°C]	250
Stagnation pressure [MPa]	1.4
Powder feed rate [g/min]	11

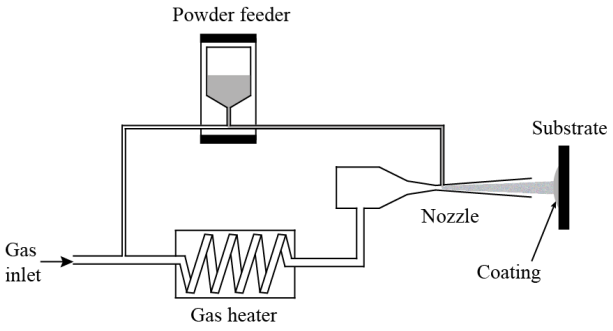

Figure 1. Schematic of the cold spray process [4].

3. Results and discussion

Thick consolidated samples with a homogenous and dense microstructure were achieved, as can be observed from figure 2A. The as-sprayed microstructure presents features typical of metal matrix composite (MMC) Cold Spray coatings, as can be observed in figure 2B, where the Al particles appear in dark grey and the CuO particles in light grey. The Al particles appear fully-deformed, while the CuO particles are agglomerated and entrapped at the interface of the Al particle boundaries. The CuO particles exhibit no significant plastic deformation, as expected considering its high hardness and brittle behavior.

Image analyses of polished samples' cross-sections have revealed porosity levels about 0.2 ± 0.1%. This low porosity level is attributed to the fact that Al particles undergo sufficient plastic deformation upon impact, no voids appear at particle–particle boundaries as a results of the Al particle deformation. Most of the porosity can be found between adjacent CuO particles due to their lack of plastic deformation upon impact. The smallest CuO particles outline the boundaries of some Al particles.

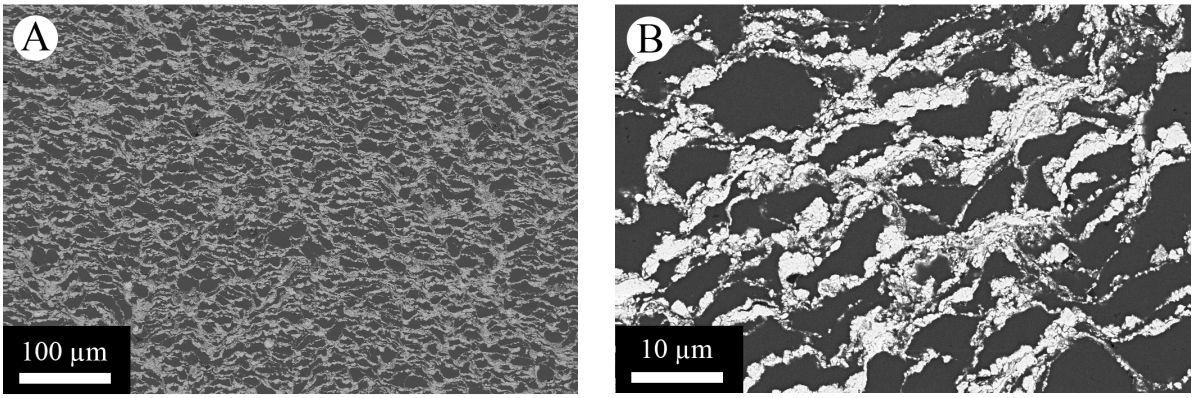

Figure 2. Cross section view of Al-CuO cold spray sample; A) low magnification, B) high magnification (Al in dark grey and CuO in light grey).

The initial mixture stoichiometry of 2Al–3CuO corresponds to a CuO volume content of 65.4%. The volume fraction of CuO in the spray consolidated samples was found to drop down to around 40 vol.%, which corresponds to a new fuel-rich mixture with an atomic ratio of 2Al–1CuO . During the spray process both Al and CuO particles are lost when some portion of the sprayed particles rebound upon impact with the substrate due to an insufficient impact velocity preventing particle deformation and bonding. Furthermore, a larger amount of CuO particles are ejected because they cannot deform due to their lack of ductility, and can only be embedded between Al particles at the interface of the particles boundaries, as observed in figure 2. Consequently, the more CuO is included in the starting powder mixture, the higher is the probability that a CuO particle hit another CuO particle and hence be ejected from the coating. Similar behavior has been observed in steel- and Al-based MMC cold sprayed coatings [9,10].

Vickers' microhardness measurements indicate a coating hardness of 115±12 kgf/mm^2 (1190±90 MPa). Small cracks appeared between CuO particle agglomerates in the vicinity of the indenter edges, but no crack propagation has been noticed in the metal matrix around the indenter print. Consequently, the metal matrix compensates the deformation by creating shear bands along the indenter print.

The four-point bending test is a simple way to subject a specimen to tension and compression simultaneously. The consolidated parts displayed an elastic behavior for strains up to 0.4%, followed by a brittle rupture, which is a typical behavior for as-sprayed cold-sprayed coatings [11]. The curves of the flexural stress versus strain exhibit a linear evolution that has been used to calculate the equivalent flexural modulus (E_f) using the equation (1) [12]:

$$E_f = \frac{{}^{\Delta F}/_{\Delta\delta} L_0^3}{8wh^3} \quad (1)$$

where, $\Delta F/\Delta\delta$ is the slope of the curve (load over extension in N/m), L_0 the initial length between support span (m), w the specimen width (m) and h the specimen thickness (m). The results of maximal flexural stress (similar to the UTS in tensile test) and the flexural modulus (equivalent to the Young' modulus) are 193±39 MPa and 46±3 GPa respectively. Typically, the samples manufactured with the cold spray process are exhibiting good mechanical properties, sufficient to keep the structural integrity of samples, as well as to machine samples even in dry conditions.

The reactivity of the mixtures has been studied through the flame propagation speed in the samples. This is commonly used to examine propagation wave behavior in solid materials such as thermites [13]. Figure 3 depicts the evolution of the deflagration speed as a function of the sample density, the two series displayed on the chart representing: *i)* the initial stoichiometric mixture 2Al−3CuO (■), which is used as a baseline; *ii)* the fuel-rich mixture 2Al-1CuO (○), corresponding to the cold spray sample stoichiometry. On this figure, the range from 25 to 85% TMD corresponds to compacted

samples, while the near-TMD value stands for the cold spray samples. First, the evolution of the flame speed starts with a quick drop between 25 to 40% density, followed by a quasi-linear decrease of the speed along the 40-85% TMD range, and finally the speed seems to remains constant between 85 to 100% TMD. It is also interesting to point out that even if the fuel-rich mixture (2:1) has a lower flame speed compared to the stoichiometric mixture (2:3), both merge together as the TMD increases.

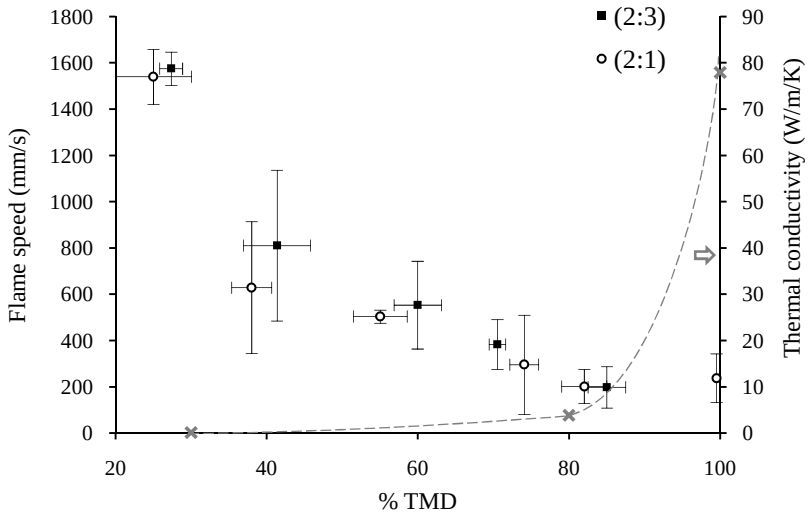

Figure 3. Flame propagation speed (○: 2Al-1CuO; ■: 2Al-3CuO) and thermal conductivity (×) versus sample relative density.

Few references from the literature have been found about the effect of porosity on the flame propagation. A recent study from Ahn et al [14] has demonstrated that the flame speed in a mixture of Al/CuO nano thermite actually follows the same trend observed in this present study. These authors have hypothesised that this evolution of the flame speed is due to the increase of thermal conductivity with the increase of TMD, although values of the thermal conductivity have not been reported.

In the present study, the thermal conductivity has been assessed for samples with 25, 80 and 100% TMD, represented by a dash line on the figure 3. Surprisingly, the sharp increase of thermal conductivity (from 3.83 to 77.88 W/m.K) occurs between 80 and 100% TMD, which does not correlate with the stagnation of the flame speed on this same range. Moreover, it has been observed in the case of gasless intermetallic reaction, that the flame speed actually follows the thermal conductivity rise with the density [15]. This behavior suggests that, in the case of thermite mixture, the thermal conduction is not the only mechanism involved into the deflagration speed drop, and the gases produced during this exothermic thermite reaction have to be considered as a second phase able to interact with the solid phase.

Focusing on the sample porosity, the literature offers extended publications in this field. The evolution of porosity in powder compacts and the percolation theory in porous media are very well described features [16]. At low density, the connected porosity is actually forming a 3-dimensionnal network of voids, which evolve during the compaction, in terms of shape, scale and tortuosity (e.g. commonly defined as the average pore path length divided by the particle size [17]). Generally, it has been noticed that this 3-D network of porosity starts collapsing around 75-80% of TMD, by turning the connected porosity into closed pores and thus decreasing drastically the gas diffusivity through the porosity.

Regarding the flame speed behavior, the range of density where the porosity is no more connected correlates closely with the percentage of TMD where the flame speed of the thermite reaction is stabilizing, at around 200 mm/s. Moreover, the image sequence from the flame speed records exhibits a different behavior of the gas phase between the loose powder (25% TMD) and the cold spray

samples (100% TMD). At low density, the deflagration wave is surrounded by a cloud of high temperature vapor, which is travelling ahead of the flame front by percolating and flowing through the porosity network and increasing the reactive surface area. In contrast, the high density samples react differently with a massive ejection of hot gas, backward of the flame, which limits the reacting area to the cross section surface. These observations are in accordance with the results obtained by Son et al [18] on the combustion of nanoscale Al/MoO_3 thermite in microchannels, where they proposed a propagation mechanism dominated by hot gas products.

4. Conclusion

The Cold Gas Dynamic Spray process has been used to consolidate a reactive thermite powder mixture, achieving a density close to the theoretical maximum density. The flame speed in unconfined samples was shown to decrease by one order of magnitude between loose powders compacted (25% TMD) and the fully dense cold-spray consolidated samples. The results suggest a transition between gas percolation/convection dominated flame propagation to conduction dominated flame propagation at vanishing porosities.

References

[1] Gotzmer C, Amato B and Kim S, 2009 Application Overview of IHDIV NSWC's Reactive Materials *Naval Sea Systems Command (NAVSEA), Naval Surface warfare Center Report*
[2] Fischer S H and Grubelich M C 1998 Theoretical energy release of thermites, intermetallics and combustible metals *24th International Pyrotechnics Seminar* Monterey CA
[3] Jouet R J, Warren A D, Rosenberg D M, Bellitto V J, Park K and Zachariah M R 2005 *Chem. Mater.* **17** 2987-96
[4] Bacciochini A, Radulescu M I, Charron-Tousignant Y, Van Dyke J, Nganbe M, Yandouzi M, Lee J J and Jodoin B 2012 *Surf. Coat. Technol.* **206** 4343-48
[5] Morris C J, Mary B, Zakar E, Barron S, Fritz G, Knio O, Weihs T P, Hodgin R, Wilkins P and May C 2010 *J. Phys. Chem. Solid,* **71** 84-89
[6] Sullivan K T, Worsley M A, Kuntz J D and Gash A E 2012 *Combust. Flame* **159** 2210-2218
[7] Alkimov A P, Kosarev V F, Nesterovich N I, and Papyrin A M 1990 *Method of Applying Coatings* Russian Patent No.1618778
[8] Davis J R 2004 *Handbook of Thermal Spray Technology* (J.R. Davis Ed., ASM International and Thermal Spray Society)
[9] Sansoucy E, Marcoux P, Ajdelsztajn L and Jodoin B 2008 *Surf. Coat. Technol.* **202** 3988-96
[10] Spencer K, Fabijanic D M and Zhang M X 2012 *Surf. Coat. Technol.* **206** 3275-82
[11] Gartner F, Stoltenhoff T, Voyer J, Kreye H, Riekehr S and Kocak M 2006 *Surf. Coat. Technol.* **200** 6770-82
[12] Grynko S 2012 *Material Properties Explained* (2nd Ed CreateSpace Independent Publishing Platform) p 38
[13] Malchi J Y, Yetter R A, Foley T J and Son S F 2008 *Combust. Sci. Technol.* **180** 1278
[14] Ahn J Y, Kim J H, Kim J M, Lee D W, Park J K, Lee D and Kim S H 2013 *Powder Technol.* **241** 67-73
[15] Akbarnejad H 2013 Influence of Porosity on the Flame Speed in Gasless Bimetallic Reactive Systems Masters' thesis University of Ottawa
[16] Sahimi M 1994 *Application of Percolation Theory* (UK/USA: Taylor & Francis Ltd) chapter 3 pp 23-39
[17] Hunt A and Ewing R 2009 *Percolation Theory for Flow in Porous Media* Lect. Notes Phys. **771** (2nd Ed Springer-Verlag, Berlin Heidelberg) chapter 10 pp 265-282
[18] Son F S, Asay B W, Foley T J, Yetter R A, Wu M H and Risha G A 2007 *J. Prop. Power* **23** 715-721